Radiance–irradiance inversion algorithm for estimating the absorption and backscattering coefficients of natural waters: homogeneous waters

Howard R. Gordon and G. Chris Boynton

A full multiple-scattering algorithm for inverting upwelling radiance (L_u) or irradiance (E_u) and downwelling irradiance (E_d) profiles in homogeneous natural waters to obtain the absorption (a) and backscattering (b_b) coefficients is described and tested with simulated data. An attractive feature of the algorithm is that it does not require precise knowledge of the scattering phase function of the medium. For the E_u–E_d algorithm, tests suggest that the error in the retrieved a should usually be $\lesssim$1%, and the error in b_b $\lesssim$10–20%. The performance of the L_u–E_d algorithm is not as good because it is more sensitive to the scattering phase function employed in the inversions; however, the error in a is usually still small, i.e., $\lesssim$3%. When the algorithm is extended to accommodate the presence of a Lambertian-reflecting bottom, the retrievals of a are still excellent, even when the presence of the bottom significantly influences the upwelling light field; however, the error in b_b can be large.

1. Introduction

Among the most common measurements in hydrologic optics are the simultaneous depth profiles of the upward and downward irradiances, E_u and E_d, or the nadir-viewing radiance, L_u and E_d. However, these are not only characteristic of the water and its constituents but also the radiance distribution incident upon the surface. In contrast, the inherent optical properties, i.e., absorption coefficient a, scattering coefficient b, and scattering phase function $P(\Theta)$, where Θ is the scattering angle, are characteristic of the medium alone.[1] These can be related to the concentration of the constituents in the medium, e.g., the chlorophyll concentration, and form the basis of the remote sensing of phytoplankton.[2] One long-standing goal of hydrologic optics has been to extract a, b, and $P(\Theta)$ from measurements of E_u and E_d. (For a complete review of this problem, see Ref. 1, Chapter 10 and the references therein.) Kirk[3,4] showed how a and b could be estimated from E_u and E_d if the correct $P(\Theta)$ for the medium were known. Gordon[5] added the variation of E_u and E_d with the solar zenith angle to estimate a, b_b, and $P(\Theta)$ for $\Theta \lesssim 40°$. Later, Gordon[6] showed that, for typical oceanic phase functions, E_u and E_d were almost unaffected by $P(\Theta)$ for $\Theta \lesssim 10$–$15°$ and only moderately affected for Θ as large as 40°. Practically this implies that, without $P(\Theta)$, b cannot be extracted from E_u and E_d, and that E_u and E_d depend mostly on a and b_b, with a minor dependence on $P(\Theta)$. This observation led us to study the possibility of an inversion algorithm that focuses on recovering a and b_b from E_u and E_d without accurate knowledge of $P(\Theta)$. Here we report the successful result of the study for a homogeneous water body. Also, as measurements of the L_u–E_d combination are now common (because of the existence of commercially available instrumentation), we report the successful extension of the algorithm to this combination and to situations in which the bottom strongly influences the light field in the water.

The authors are with the Department of Physics, University of Miami, Coral Gables, Florida 33124.

Received 7 June 1996; revised manuscript received 7 October 1996.

0003-6935/97/122636-06$10.00/0

2. Algorithm and Its Performance

The algorithm is capable of using either $E_d(z)$ and $E_u(z)$ or $E_d(z)$ and $L_u(z)$. We begin by describing the operation in the former case. We assume that E_u and E_d are provided at N depths denoted by z_i, and

that N is large enough so that depth derivatives of these quantities can be accurately computed.

A. E_u–E_d Algorithm

To start the E_u–E_d algorithm, one must have initial guesses for a and b_b. These are estimated in the following manner. If the scalar irradiance $E_0(z)$ were measured, the absorption coefficient could be determined from Gershun's law,[1] i.e.,

$$a(z) = \bar{\mu}(z) K_E(z), \tag{1}$$

where $\bar{\mu}(z)$ is the average cosine of the radiance distribution, $\bar{\mu} \equiv (E_d - E_u)/E_0$, and $K_E \equiv -d/dz[ln(E_d - E_u)]$ is the attenuation coefficient of the vector irradiance. In the absence of E_0, we simply estimate $\bar{\mu}$ to be μ_0, the cosine of the solar zenith angle (θ_0') measured in the water. Thus, the initial guess for a is $a^{(0)}(z) = \mu_0 K_E(z)$. As we assume that the medium is homogeneous, we average $a^{(0)}(z)$ over depth, weighed by a function $f(z)$, to obtain the absorption coefficient characteristic of the medium as a whole, i.e.,

$$a^{(0)} = \frac{\int_0^{z_m} a^{(0)}(z) f(z) \mathrm{d}z}{\int_0^{z_m} f(z) \mathrm{d}z}, \tag{2}$$

where z_m is the maximum depth of the measurements. We use a weighting in which $f(z) = ln[E_d(z)]$, which because $E_d(z)$ has a near-exponential decay with z, yields a near-linear weighting with depth, i.e., deeper measurements are weighed more heavily than surface measurements. Other weightings work equally well; however, we prefer this, as the measured values of E_d near the surface are likely to be the least accurate because of ship shadowing and wave-induced irradiance fluctuations.

The initial estimate of $b_b(z)$ is obtained from the irradiance ratio, $R(z) \equiv E_u(z)/E_d(z)$, by using the well-known approximation for R near the surface,[7,8] $R \approx 0.33 b_b/a$, so $b_b{}^{(0)}(z) = 3R(z)a^{(0)}$. This guess for $b_b{}^{(0)}(z)$ is then averaged over depth in a manner identical to $a^{(0)}(z)$ to obtain $b_b{}^{(0)}$.

A scattering phase function $P(\Theta)$, where Θ is the scattering angle, is now assumed for the medium. From P and b_b it is possible to estimate the scattering coefficient b through

$$\tilde{b}_b \equiv \frac{b_b}{b} = 2\pi \int_{\pi/2}^{\pi} P(\Theta) \sin\Theta \cos\Theta \, \mathrm{d}\Theta.$$

Thus $b_b{}^{(0)}$ provides an initial estimate of b, i.e., $b^{(0)}$. The beam attenuation coefficient of medium c is then estimated as $c^{(0)} = a^{(0)} + b^{(0)}$.

The initial guesses $a^{(0)}$, $b^{(0)}$, and $c^{(0)}$ along with $P(\Theta)$ are entered into the radiative transfer equation (RTE), the solution of which provides all the irradiances, $E_d{}^{(0)}(z)$, $E_u{}^{(0)}(z)$, and $E_0{}^{(0)}(z)$. These are used to form $R^{(0)}(z) \equiv E_u{}^{(0)}(z)/E_d{}^{(0)}(z)$ and $\bar{\mu}^{(0)}(z) \equiv [E_d{}^{(0)}(z) - E_u{}^{(0)}(z)]/E_0{}^{(0)}(z)$. A new estimate for a is then made by using $a^{(1)}(z) = \bar{\mu}^{(0)}(z) K_E(z)$, and the error $\Delta R(z) \equiv R(z) - R^{(0)}(z)$ is determined. This error in $R^{(0)}(z)$ is then used to estimate the error in b_b through $\Delta b_b(z) = 3\Delta R(z) a^{(1)}(z)$. This is used to form a new estimate for $b_b(z)$: $b_b{}^{(1)}(z) = b_b{}^{(0)}(z) + \epsilon \Delta b_b(z)$, where ϵ is a constant between zero and one that determines the speed of convergence and the stability of the iteration. We typically choose ϵ to be 0.25.

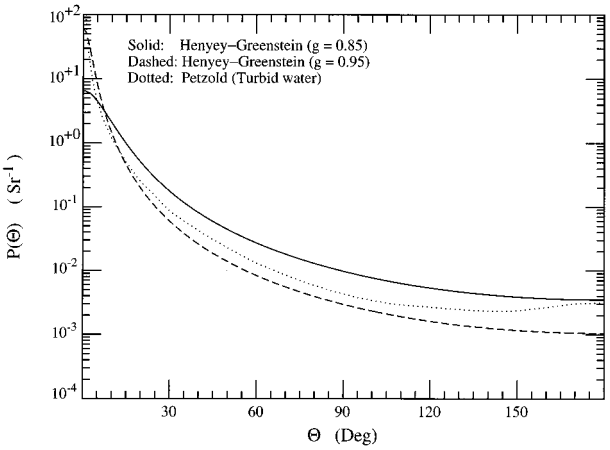

Fig. 1. Scattering phase functions used in this study (normalized to unity).

Then, just as $b^{(0)}$ and $c^{(0)}$ were determined from $a^{(0)}$ and $b_b{}^{(0)}$, $b^{(1)}$ and $c^{(1)}$ are determined from $a^{(1)}$ and $b_b{}^{(1)}$. These are then reintroduced into the RTE to determine a new estimate for the irradiances, i.e., $E_d{}^{(1)}(z)$, $E_u{}^{(1)}(z)$, and $E_0{}^{(1)}(z)$. The iteration process then continues with the nth + 1 iteration following the nth iteration in exactly the same manner as the first iteration followed the zeroth iteration above. The algorithm is stopped when the residual error after n iterations, defined as

$$\delta^{(n)} = \frac{1}{N}\sum_{i=1}^{N} |\ln[E_d{}^{(n)}(z_i)] - \ln[E_d(z_i)]| + \frac{1}{N}\sum_{i=1}^{N} \times |\ln[E_u{}^{(n)}(z_i)] - \ln[E_u(z_i)]|,$$

reaches a minimum.

B. Tests of the E_u–E_d Algorithm

To test this algorithm, we assume an infinitely deep medium with $c = 1\ \mathrm{m}^{-1}$. The scattering coefficient was then varied from 0.2 to 0.95 m^{-1}, implying that the single-scattering albedo of the medium, $\omega_0 \equiv b/c$, varied from 0.2 to 0.95. The scattering phase function for the medium was taken to be a one-term Henyey–Greenstein[9] (HG) function with asymmetry parameter $g = 0.85$ (Fig. 1). The irradiance pseudodata were created at 0.25-m depths from the surface to 4.75 m, i.e., from the surface to 4.75 optical depths, by a Monte Carlo radiative transfer code in which the ocean could be illuminated with the solar beam alone (no atmosphere), the solar beam and skylight from a

Table 1. Test of the E_u–E_d Algorithm with a Correct and Incorrect $P(\Theta)$ used in the Inversion

Source[a] (deg)	ω_0	Correct $P(\Theta)$[b] δa (%)	Correct $P(\Theta)$[b] δb_b (%)	Incorrect $P(\Theta)$[b] δa (%)	Incorrect $P(\Theta)$[b] δb_b (%)
0	0.20	+0.6	−0.4	+0.3	−1.7
0	0.40	+0.4	+0.9	−0.5	−4.4
0	0.60	+0.2	+0.4	−1.0	−7.5
60	0.60	+0.1	+0.2	−0.8	−7.4
D	0.60	+0.3	+0.6	−0.9	−7.5
0	0.80	−0.3	−0.4	−0.6	−9.4
0	0.90	+0.2	+0.2	−0.2	−10.2
0	0.95	−0.1	−0.3	−1.0	−10.5
60	0.95	+0.1	+0.9	−0.5	−9.5
D	0.95	−0.1	+0.1	−0.4	−10.0

[a]Here 0° and 60° mean the source is the Sun at solar zenith angles of 0° and 60°, respectively; D indicates totally diffuse radiance incident upon the surface.
[b]δa and δb_b are the errors in the retrieved values of a and b_b, respectively.

50-layer atmosphere containing both aerosol and Rayleigh scattering, or by a uniform radiance distribution used to simulate illumination under overcast skies. The code has been thoroughly tested and compares favorably with other radiative transfer codes used in hydrologic optics.[10] A similar radiative transfer code was used as a subroutine to solve the RTE at each iteration in the inversion process.

Table 1 provides the results of a test of the algorithm for a case in which the correct phase function for the medium was used in the inversion process. In this case the atmosphere was absent and the solar zenith angle θ_0 (in air) was either 0 or 60°. Two cases of a uniform incident distribution (to simulate overcast conditions) are also included. The same incident radiance distribution is used in both the code for generating the pseudodata and the inversion code. Table 1 shows that the maximum error in the retrieved values of a and b_b is $\lesssim$1% when the correct phase function is employed. It also shows that the algorithm works equally well under a variety of incident radiance distributions.

When an incorrect phase function is used with the same pseudodata, the error in b_b increases; however, the error in a remains small. This is also shown in Table 1. In this case a HG phase function with $g = 0.95$ (Fig. 1) was assumed in the inversion process. It should be pointed out that this error in the assumed phase function is very large: b_b/b, the backscattering probability, is 0.036 and 0.011 for $g = 0.85$ and 0.95, respectively. The assumed phase function underestimates the backscattering probability by more than a factor of 3; however, the maximum error in the retrieved b_b is still only −12%. The algorithm compensates for the too-small values of b_b/b by increasing b until a nearly correct b_b is found.

Note that, for a given ω_0, the results in Table 1 are applicable to any value of c if z_i is replaced by cz_i, the optical depth corresponding to z_i.

For a final test of the E_u–E_d algorithm, we inverted the irradiance data obtained from Tyler's[11,12] measurements of the radiance distribution at 480 nm as a function of depth in Lake Pend Oreille, Idaho, under conditions of optical homogeneity throughout the water column. As the full radiance distribution was measured, it was possible to obtain $E_u(z)$, $E_d(z)$, and $E_0(z)$ and therefore to use Gershun's law to obtain the true value of a. The result ranged from 0.112 to 0.118 m^{-1} with a mean of ~0.116 m^{-1}.[13] The variation in the derived value of a may be due to a weak vertical structure in the water column not seen in the beam transmittance, e.g., a minimum in $R(z)$ was observed near $z = 10$ m. Using only the $E_u(z)$ and $E_d(z)$ values, we employed our algorithm with an aerosol-free, Rayleigh-scattering atmosphere over the lake and a HG phase function with various values of g for the water. The resulting retrieved values of a and b_b are provided in Table 2. All the retrieved values of a are within ~4% of the value computed from Gershun's law, and the retrieved values of a and b_b are only weak functions of g. Unfortunately, no measurements were made from which b_b could be obtained for comparison; however, from the measured value of c (0.402 m^{-1}), one finds $b = 0.281$ m^{-1}, which combined with our b_b yields $\tilde{b}_b = 0.020$–0.022, not unreasonable values.

Table 2. Test of the Algorithms with Tyler's Radiance Data

Algorithm	g[a]	a[b] (m^{-1})	b_b (×1000) (m^{-1})
E_u–E_d	0.85	0.1203	6.18
E_u–E_d	0.90	0.1183	5.98
E_u–E_d	0.95	0.1174	5.70
L_u–E_d	0.85	0.1178	6.71
L_u–E_d	0.90	0.1167	6.46
L_u–E_d	0.95	0.1148	6.38
E_u, E_d, E_0	—	0.116	—

[a]g is the HG g value used in the inversion algorithm.
[b]a is determined from Gershun's law.

C. L_u–E_d Algorithm

When the algorithm is operated with $E_d(z)$ and $L_u(z)$, the procedure is basically the same. L_u and E_u are related by the Q factor[14]: $Q \equiv E_u/L_u$. The Q factor usually ranges from approximately 3 to 6, and for a totally uniform radiance distribution $Q = \pi$. If we knew the value of Q, we could find E_u from L_u and operate the algorithm in the same manner as above with E_u. That was our strategy. Briefly, an initial estimate of E_u was obtained by assuming that L_u is totally diffuse, i.e., $Q = \pi$. This was then used in the algorithm above to compute not only $E_d^{(0)}(z)$, $E_u^{(0)}(z)$, and $E_0^{(0)}(z)$, but also $L_u^{(0)}(z)$. This provides a better estimate of Q, i.e., $Q^{(0)}(z) = E_u^{(0)}(z)/L_u^{(0)}(z)$. The revised estimate of Q is then used to provide a more realistic estimate of E_u, which is used in the algorithm as before. Thus, at each iteration, not only are

Table 3. Test of the L_u–E_d Algorithm with a Correct and Incorrect $P(\Theta)$ used in the Inversion

Source[a] (deg)	ω_0	Correct $P(\Theta)$[b] δa (%)	Correct $P(\Theta)$[b] δb_b (%)	Incorrect $P(\Theta)$[b] δa (%)	Incorrect $P(\Theta)$[b] δb_b (%)
0	0.20	+0.7	−0.6	+0.3	−1.9
0	0.40	+0.6	+0.6	−0.6	−5.2
0	0.60	+0.1	+0.1	−1.7	−4.5
60	0.60	+0.1	−0.3	−1.5	−4.1
D	0.60	+0.3	+0.3	−1.6	−4.7
0	0.80	−0.2	−0.2	−1.6	−8.0
0	0.90	−0.2	−0.3	−0.6	−7.2
0	0.95	−0.0	−0.9	−1.5	−9.9
60	0.95	−0.1	+0.3	−0.7	−9.4
D	0.95	+0.2	−0.0	−0.2	−7.8

[a]Here 0° and 60° mean the source is the Sun at solar zenith angles of 0° and 60°, respectively; *D* indicates totally diffuse radiance incident upon the surface.
[b]δa and δb_b are the errors in the retrieved values of a and b_b, respectively.

the values of a and b_b updated; the values of E_u are updated as well. As before the calculation stops when the agreement between the computed and measured values of $L_u(z)$ and $E_d(z)$ are as close as the algorithm can achieve.

D. Tests of the L_u–E_d Algorithm

The results of simulations in which L_u and E_d, generated with a HG phase function ($g = 0.85$), are used as input pseudodata and the retrieval of a and b_b carried out by using a correct or an incorrect (HG, $g = 0.95$) phase function are provided in Table 3. The agreement is seen to be as good as that seen in Table 1 for the E_u and E_d pseudodata. However, noting that in the quasi-single-scattering approximation[15,16]

$$L_u \propto \frac{P(\pi - \theta_0')}{1 + \mu_0},$$

i.e., that L_u is directly proportional to the phase function evaluated at $\pi - \theta_0'$, and that the HG phase functions with $g = 0.85$ and 0.95 have similar shapes for $\Theta > 90°$ (Fig. 1), we believed it was important to see how the algorithm would perform with pseudodata created with a measured aquatic phase function (Petzold's[17] turbid-water phase function shown in Fig. 1) that does not have the HG shape. Petzold's phase function has the property that it is close to a HG with $g = 0.95$ for $\Theta \lesssim 90°$, and closer to a HG with $g = 0.85$ for scattering angles near 180°. Thus, for θ_0 near 0°($\theta_0' \approx 0°$), using a HG with $g = 0.85$ in the retrieval algorithm would be expected to lead to reasonable results, as the Petzold and HG($g = 0.85$) phase functions have similar values near $\Theta \approx 180°$. In contrast, for larger values of θ_0 (larger θ_0') we would expect significant error in the retrieved b_b, as the two phase functions can differ by as much as a factor of 2. These expectations are confirmed by Table 4, which provides the error in a and b_b retrieved from both the E_u–E_d and L_u–E_d algorithms when the pseudodata were created by using Petzold's phase function and the retrieval was carried out by using a HG with $g = 0.85$. The L_u–E_d algorithm yields a large error in the retrieved b_b, and the error increases with increasing θ_0. However, it is important to note that even with the unrealistic phase function used in these retrievals (HG), the L_u–E_d algorithm still usually yielded an a with only a few percent error. Interestingly, the E_u–E_d algorithm still produces excellent retrievals for a, and the b_b retrievals are in error by $\lesssim$20%. Of course, there is no reason that the algorithm could not be operated by using a more realistic phase function in place of the HG phase function, which we used here solely for convenience.

Table 4. Test of E_u–E_d and L_u–E_d Algorithms[a]

Source[b] (deg)	ω_0	E_u–E_d[c] δa (%)	E_u–E_d[c] δb_b (%)	L_u–E_d[c] δa (%)	L_u–E_d[c] δb_b (%)
0	0.20	+0.6	−15.3	−1.2	+31.6
60	0.20	+1.2	−18.6	+0.8	−56.0
0	0.60	+0.2	−15.9	−2.9	+6.6
60	0.60	−0.6	−19.8	+3.5	−52.8
0	0.80	−0.2	−17.9	−3.3	−7.1
60	0.80	−0.4	−19.5	+7.8	−50.0

[a]Here the Petzold phase function is used to create the pseudodata, and a HG with $g = 0.85$ is used in the retrievals.
[b]Here 0° and 60° mean the source is the Sun at solar zenith angles of 0° and 60°, respectively.
[c]δa and δb_b are the errors in the retrieved values of a and b_b, respectively.

Finally, we also tested the L_u–E_d algorithm by using the radiance distribution from Lake Pend Oreille,[11,12] and a Rayleigh-scattering atmosphere. The results are provided in Table 2 and are similar to those for the E_u–E_d algorithm. To see if the pure Rayleigh-scattering atmosphere assumption has a significant effect on the results, we carried out additional tests of the algorithm with a moderate amount of aerosol in the atmosphere (aerosol optical thickness of 0.25 at 480 nm). These yielded essentially the same results as those given in Table 2, e.g., for $g = 0.85$, the retrieved values of a and b_b were 0.1175 and 6.84×10^{-3} m^{-1}, respectively, suggesting that the aerosol concentration has little effect on the retrieval of a and b_b.

3. Presence of a Reflecting Bottom

We have modified this algorithm to accommodate the existence of a Lambertian-reflecting surface at the bottom of the medium. For moderate surface albedos (A_B), the presence of the bottom can significantly change the upwelling light field in the water column, e.g., L_u and E_u can even increase with depth. Thus, in the presence of the bottom, the algorithm uses $f(z) = E_d(z)$ in Eq. (2), as the equation relating $b_b(z)$ to the irradiances is more appropriate near the surface where the perturbation caused by the bottom is smallest. Also, as the equations for determining $a^{(0)}(z)$ and $b_b{}^{(0)}(z)$ are likely to be quite inaccurate, we simply start the algorithm with $\omega_0 = 0.5$. Table 5

Table 5. Test of the L_u–E_d Algorithm with a Correct and Incorrect $P(\Theta)$ used in the Inversion[a]

		z_B = 3.00 m				z_B = 4.75 m			
		Correct $P(\Theta)$		Incorrect $P(\Theta)$		Correct $P(\Theta)$		Incorrect $P(\Theta)$	
ω_0	A_B	δa (%)	δb_b (%)	δa (%)	δb_b (%)	δa (%)	δb_b (%)	δa (%)	δb_b (%)
0.20	0.25	+0.0	+34.3	−1.0	+37.5	+0.3	+8.9	+0.2	+8.3
0.20	0.50	−1.3	+55.5	−2.4	+81.3	+0.2	+11.0	+0.1	+18.8
0.20	1.00	−3.3	+127.6	−0.0	+17.5	+0.3	+19.7	−0.7	+23.0
0.60	0.25	−0.2	−0.7	−2.3	+4.3	+0.4	+0.6	−1.6	−0.9
0.60	0.50	−0.3	+2.7	−2.0	+3.0	−0.5	+5.1	−1.5	−0.5
0.60	1.00	+1.3	+15.3	−2.0	−1.1	−0.4	+2.4	−2.8	+5.8
0.80	0.25	+0.1	+0.3	−2.9	+6.0	+0.2	+1.0	−1.5	−3.2
0.80	0.50	−1.2	+9.2	−4.8	+19.5	−0.5	+4.1	−3.0	+2.2
0.80	1.00	+7.9	−52.2	−1.6	+3.1	−0.7	+4.0	+1.4	−14.7

[a]The solar zenith angle is 0°, the bottom depth is z_B, and the bottom albedo is A_B.

provides the results of this algorithm operated with L_u and E_d for a medium with $c = 1\ \mathrm{m}^{-1}$ and bottom depths (z_B) of 3.00 and 4.75 m. As in Tables 1 and 3, the Henyey–Greenstein asymmetry parameter was 0.85 for the correct $P(\Theta)$ and 0.95 for the incorrect $P(\Theta)$. The correct value of A_B was used in the retrieval algorithm, as it can be measured along with L_u and E_d. The results clearly show that the absorption coefficient can usually be accurately retrieved from the pseudodata; however, large errors in b_b can occur if the bottom albedo is large and z_B is small. An appreciation for the magnitude of the influence of the bottom on the light field in these simulations can be obtained from Fig. 2, which compares the true values of $L_u(z)$ (filled circles) and the values obtained by using the retrieved optical properties (solid curves) for z_B = 4.75 m and A_B = 1.0, along with similar curves for the case of an infinitely deep medium (open circles and dotted curves) with identical optical properties. Near the bottom, for $\omega_0 = 0.2$, L_u is ~3 orders of magnitude larger in the presence of the bottom than it would be in its absence. Note that, for ω_0 = 0.2 in the presence of the bottom, examination of the graph would lead one to conclude that the retrieved value of b_b was too large. Thus, one could obtain an improved b_b simply by reducing it manually enough to provide a better fit to the data.

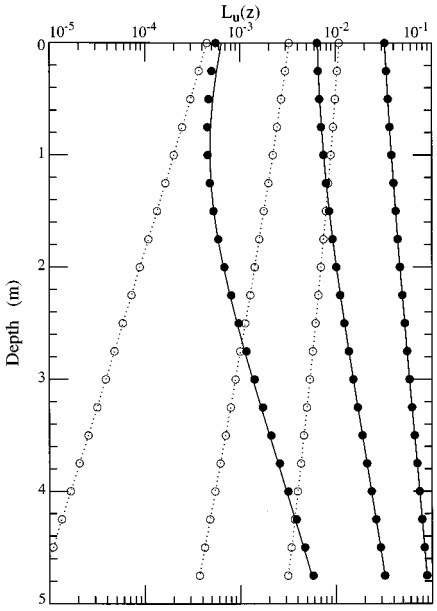

Fig. 2. Comparison between the true upwelling radiance (filled circles) and the values obtained by using the retrieved inherent optical properties (solid curves) in the presence of a reflecting bottom ($z_B = 4.75, A_B = 1.0$), using the correct $P(\Theta)$. Curves from left to right correspond to ω_0 = 0.2, 0.6, and 0.8. The corresponding cases for an infinitely deep medium are provided by the open circles and the dotted curves.

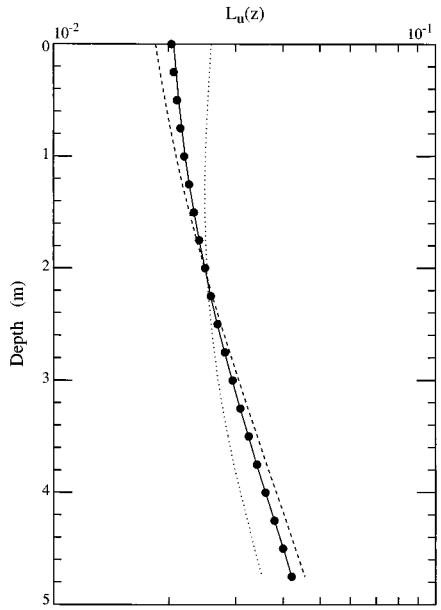

Fig. 3. Example of the fit of L_u to the pseudodata when an incorrect value of A_B is used in the retrievals. Here $\omega_0 = 0.8, g = 0.85$ (used to create the pseudodata and to operate the inversion algorithm), z_B = 4.75 m, and the true A_B was 0.5. The filled circles provide the $L_u(z)$ pseudodata using these parameters. The dotted, solid, and dashed curves are the L_u profiles obtained by using the retrieved inherent optical properties with A_B = 0.45, 0.50, and 0.55, respectively, used in the inversion algorithm.

We also operated the algorithm with a ±10% error in A_B, i.e., the value of A_B assumed in the retrieval algorithm differed by the true A_B (used in creating the pseudodata) by ±10%. Of course, the errors in the retrieval of a and b_b were larger; however, a comparison of the resulting $L_u(z)$, derived by using the retrieved values of a and b_b, with the $L_u(z)$ pseudodata showed that a very poor fit was obtained in these cases (Fig. 3), clearly indicating that the bottom albedo was incorrect.

4. Concluding Remarks

In conclusion, we have provided an iterative algorithm for inverting either the E_u–E_d or L_u–E_d pair to obtain the absorption and backscattering coefficients of a homogeneous medium bounded by a Lambertian-reflecting bottom. The algorithm employs complete multiple-scattering solutions to the radiative transfer equation. An attractive feature of the algorithm is that it does not require precise knowledge of $P(\Theta)$.

The algorithm was validated for both a and b_b by using simulated radiance–irradiance data for which the correct values of the coefficients were known (Tables 1, 3, 4, and 5), and for a by using an experimentally measured radiance distribution from Lake Pend Oreille, Idaho (Table 2).

The algorithm usually provided an excellent retrieval of a (error $\lesssim$1%), even when the phase function used in the retrievals departed considerably from the true phase function (Fig. 1). The error in b_b was larger; however, it was usually $\lesssim$10%. Typically, the error in both a and b_b will be significantly reduced if the phase function used in the retrieval is close to the actual phase function (Tables 1, 3, and 4). As expected, the L_u–E_d algorithm was more sensitive to the choice of the phase function used in the retrievals than the E_u–E_d algorithm. In cases in which the influence of the bottom caused a strong perturbation to the light field (Fig. 2), the error in a usually remained small, but the error in b_b could become large (Table 5).

As these retrieval algorithms ignore inelastic scattering,[18–20] they should not be applied to spectral regions in which inelastic scattering can make a significant contribution to the irradiances, e.g., in the red, unless the contribution from inelastic processes is assessed.[21]

The authors are grateful to the U.S. Office of Naval Research for support under grant N00014-89-J-1985.

References

1. C. D. Mobley, *Light and Water; Radiative Transfer in Natural Waters* (Academic, New York, 1994).
2. H. R. Gordon and A. Y. Morel, *Remote Assessment of Ocean Color for Interpretation of Satellite Visible Imagery: A Review* (Springer-Verlag, New York, 1983).
3. J. T. O. Kirk, "Estimation of the scattering coefficient of natural waters using underwater irradiance measurements," Aust. J. Mar. Freshwater Res. **32,** 533–539 (1981).
4. J. T. O. Kirk, "Estimation of the absorption and scattering coefficients of natural waters by the use of underwater irradiance measurements," Appl. Opt. **33,** 3276–3278 (1994).
5. H. R. Gordon, "Absorption and scattering estimates from irradiance measurements: Monte Carlo simulations," Limnol. Oceanogr. **36,** 769–777 (1991).
6. H. R. Gordon, "Sensitivity of radiative transfer to small-angle scattering in the ocean: a quantitative assessment," Appl. Opt. **32,** 7505–7511 (1993).
7. H. R. Gordon, O. B. Brown, and M. M. Jacobs, "Computed relationships between the inherent and apparent optical properties of a flat homogeneous ocean," Appl. Opt. **14,** 417–427 (1975).
8. A. Morel and L. Prieur, "Analysis of variations in ocean color," Limnol. Oceanogr. **22,** 709–722 (1977).
9. G. W. Kattawar, "A three-parameter analytic phase function for multiple scattering calculations," J. Quant. Spectrosc. Radiat. Transfer **15,** 839–849 (1975).
10. C. D. Mobley, B. Gentili, H. R. Gordon, Z. Jin, G. W. Kattawar, A. Morel, P. Reinersman, K. Stamnes, and R. H. Stavn, "Comparison of numerical models for computing underwater light fields," Appl. Opt. **32,** 7484–7504 (1993).
11. J. E. Tyler, "Radiance distribution as a function of depth in an underwater environment," Bull. Scripps Inst. Oceanogr. **7,** 363–411 (1960).
12. J. E. Tyler and R. W. Preisendorfer, "Transmission of energy within the sea: light," in *The Sea*, M. N. Hill, ed. (Interscience, New York, 1962) pp. 397–451.
13. R. W. Preisendorfer, "Application of radiative transfer theory to light measurements in the sea," Union Geodes. Geophys. Int. **10,** 11–30 (1961).
14. R. W. Austin, "The remote sensing of spectral radiance from below the ocean surface," in *Optical Aspects of Oceanography*, N. G. Jerlov and E. S. Nielsen, eds. (Academic, London, 1974) pp. 317–344.
15. H. R. Gordon, "Simple calculation of the diffuse reflectance of the ocean," Appl. Opt. **12,** 2803–2804 (1973).
16. H. R. Gordon, "Modeling and simulating radiative transfer in the ocean," in *Ocean Optics*, R. W. Spinrad, K. L. Carder, and M. J. Perry, eds. (Oxford U. Press, Oxford, 1994), pp. 3–39.
17. T. J. Petzold, "Volume scattering functions for selected natural waters," SIO Ref. 72–78 (Scripps Institution of Oceanography, Visibility Laboratory, San Diego, Calif., 1972).
18. R. H. Stavn and A. D. Weidemann, "Optical modeling of clear ocean light fields: Raman scattering effects," Appl. Opt. **27,** 4002–4011 (1988).
19. B. R. Marshall and R. C. Smith, "Raman scattering and in-water ocean optical properties," Appl. Opt. **29,** 71–84 (1990).
20. T. G. Peacock, K. L. Carder, C. O. Davis, and R. G. Steward, "Effects of fluorescence and water Raman scattering on models of remote sensing reflectance," in *Ocean Optics X*, R. W. Spinrad, ed., Proc. SPIE **1302,** 303–319 (1990).
21. Y. Ge, K. J. Voss, and H. R. Gordon, "In situ measurements of inelastic scattering in Monterey Bay using solar Fraunhofer lines," J. Geophys. Res. **100,** 13,227–13,236 (1995).